Original Article

Comparison of different processed products of *Allium tuberosum Rottler* for the treatment of mice asthenozoospermia

Wenhui Wu[1#], Xiaohong Guo[1#], Jie Li[1], Min Yang[1], Yongai Xiong[2]

[1]Institute of Chinese Pharmaceutical Preparations, Chongqing Traditional Chinese Medicine Hospital, Chongqing, China; [2]Key Laboratory of Basic Pharmacology of Guizhou Province and School of Pharmacy, Zunyi Medical University, Zunyi, China

Contributions: (I) Conception and design: Y Xiong, M Yang; (II) Administrative support: All authors; (III) Provision of study materials or patients: None; (IV) Collection and assembly of data: W Wu, X Guo; (V) Data analysis and interpretation: J Li; (VI) Manuscript writing: All authors; (VII) Final approval of manuscript: All authors.

[#]These authors contributed equally to this work.

Correspondence to: Yongai Xiong, MD, PhD. Key Laboratory of Basic Pharmacology of Guizhou Province and School of Pharmacy, Zunyi Medical University, Road 1, Campus, Xinpu New District, Zunyi 563000, China. Email: yaxiong@zmu.edu.cn; Min Yang, BS. Institute of Chinese Pharmaceutical Preparations, Chongqing Traditional Chinese Medicine Hospital, No. 6, Panxi 7 Branch Road, Jiangbei District, Chongqing 400021, China. Email: cqyangmin@126.com.

Background: *Allium tuberosum Rottler* improves sexual function and is used in the treatment of impotence and spermatorrhea. However, its chemical composition and mechanism of action remain unclear. This study investigates the chemical composition and mechanism of action of *Allium tuberosum Rottler* co-processed with salt and wine (GZP) in modulating testicular mitochondrial autophagy for the treatment of asthenozoospermia in mice.

Methods: Adenine gavage + cyclophosphamide intraperitoneal injection was used to establish the model of asthenozoospermia, and six *Allium tuberosum Rottler* processed products were compared in the pharmacological efficacy for the treatment of asthenozoospermia in mice. The liquid chromatograph mass spectrometer (LC-MS) assay was performed to analyse the compositional changes in the GZP. The mechanism of GZP in the treatment of asthenozoospermia in mice was further investigated. The mitophagy was detected by transmission electron microscope (TEM) and immunofluorescence, respectively. Reactive oxygen species (ROS) were detected by probe. Protein expression was determined by Western blotting.

Results: GZP exhibited optimal therapeutic effects on asthenozoospermia in mice. It showed the best therapeutic effect in improving the total number of spermatozoa, sperm survival rate, improving sperm viability and reducing sperm deformity rate, alleviating the abnormal pathological morphology of mice testis, and increasing the serum testosterone (T), follicle-stimulating hormone (FSH) and prolactin (PRL) levels in mice. The LC-MS detection found that Allicin showed the most significant increase in GZP. Besides, GZP reduced ROS level and inhibited mitophagy in mice testicular tissues. Meanwhile, it restrained the expression of PINK1, Parkin, Light chain 3II (LC3-II)/Light chain 3I (LC3-I) and Caspase-3 proteins.

Conclusions: GZP improves asthenozoospermia via inhibiting excessive mitophagy and protects the integrity of mitochondria by blocking the PINK1/Parkin signaling pathway. During which, the Allicin may play an important role.

Keywords: Asthenozoospermia; *Allium tuberosum Rottler*; Allicin; mitophagy

Submitted Jun 06, 2024. Accepted for publication Oct 11, 2024. Published online Oct 28, 2024.
doi: 10.21037/tau-24-274
View this article at: https://dx.doi.org/10.21037/tau-24-274

Introduction

Asthenozoospermia is defined as the reduction or absence of motile spermatozoa in male ejaculate, with a lower reference value established by the World Health Organization of 40% of total motile sperm and 32% of progressive sperm and a total sperm motility lower than 40% and a progressive sperm motility lower than 32% in a semen sample (1,2). According to Shahrokhi *et al.* (3), spermatozoa with grade a + b (Sperm Class a and Sperm Class b) less than 50% or spermatozoa with grade a less than 25% nonetheless meet the definition requirements used by some hospitals and research institutes. This is mostly due to the spermatozoa's poor ability to move ahead. At present, the pathogenesis of weak spermatozoa has not been completely clarified, and the incidence of male infertility is increasing year by year. The causative factors of male infertility are complex, and both endogenous and exogenous factors can affect sperm quality, and oligo asthenozoospermia is an important factor contributing to male infertility (4). The etiology of asthenozoospermia is complex and is associated with environmental factors, occupational exposures, chromosomal abnormalities, gene deletions, infections, endocrine factors, semen insufficiency, certain immune factors, varicocele, micronutrient deficiencies, and medical disorders (5). Furthermore, antitumour drugs are being used more often in clinics due to the gradual increase in cancer incidence. Certain antitumour drugs, like cyclophosphamide, leucovorin, cisplatin, etc., have reproductive toxicity on patients receiving treatment, which lowers sperm quality and decreases fertility in male patients (5). For example, male subjects treated with cyclophosphamide exhibit oligozoospermia or azoospermia, as well as biochemical and histological changes in the testes and epididymis, showing disorders of sex hormone secretion and low blood testosterone levels and testicular damage (6). Currently, western medicine mostly uses empirical drugs to treat asthenozoospermia, which is idiopathic male infertility. These treatments are clinically ineffective in treating oligozoospermia (3). Although conventional treatments such as medication, surgery, and assisted reproductive technology have helped many couples with fertility problems achieve clinical pregnancy, these treatments are efficacious, however, they are invasive, expensive, and associated with adverse effects and other risks (7). In contrast, traditional Chinese medicine (TCM) has long been used in the treatment of male infertility and has a unique role in the treatment of male infertility with therapeutic effects (8).

Allium tuberosum Rottler is the dried mature seeds of leek (*Allium tuberosum RottL.ex Spreng.*) of the lily family, which mainly contains fatty acids, volatile oil, saponins, nucleosides, alkaloids, flavonoids, active peptides, sulphides and other chemical compositions (9). Numerous studies have shown that *Allium tuberosum Rottler* have a variety of pharmacological activities such as improving sexual function, protecting the liver, improving immunity, antioxidant, antibacterial, etc., which can be used to treat intractable eruption, tooth decay pain, impotence and spermatorrhea, frequent urination, lumbar and knee pain and so on (10,11). *Allium tuberosum Rottler* have a long history in traditional Chinese herbal medicine, and it usually requires special treatment before it can be used. For example, *Allium tuberosum Rottlers* are processed with salt, wine, vinegar and so on, and the chemical composition of *Allium tuberosum Rottlers* obtained by different processing methods varies considerably. However, at present, there is no literature report on the use of *Allium tuberosum Rottler* and its processed products in the treatment of asthenospermia.

Mitophagy, an important mitochondrial quality control mechanism, leads to the gradual accumulation of mitochondrial DNA (mitochondrial DNA, mtDNA) mutations in response to stresses such as reactive oxygen species (ROS) stress, as well as reduced intracellular

Highlight box

Key findings

- *Allium tuberosum Rottler* co-processed with salt and wine (GZP) exhibits optimal therapeutic effects on asthenozoospermia in mice.
- Allicin may be the main active ingredient in GZP.
- GZP reduce reactive oxygen species (ROS) level and inhibit mitophagy in mice testicular tissues.

What is known and what is new?

- *Allium tuberosum Rottler* improves sexual function and is used in the treatment of impotence and spermatorrhea, its chemical composition and mechanism of action remains unclear.
- Our study shows that GZP effectively ameliorate asthenozoospermia in mice, and it may inhibit excessive autophagy and protect the integrity of mitochondria by blocking the PINK1/Parkin signaling pathway, and ultimately alleviate the mitochondrial disorders in the testis tissues of mice to inhibit their apoptosis.

What is the implication, and what should change now?

- This study's findings provide important evidence for the use of *Allium tuberosum Rottler* in the treatment of asthenozoospermia.
- To facilitate this shift, there should be a concerted effort to expand clinical use of *Allium tuberosum Rottler*.

mitochondrial membrane potential and depolarisation damage, and ultimately cell death (12,13). It is reported that testicular mitochondrial function has an important effect on spermatozoa (14,15). Asthenospermia has been linked to reduced numbers of mitochondrial gyres, aberrant mitochondrial assembly, or structural flaws in mitochondrial membranes. The metabolism that spermatozoa employ to utilise the various energy sources available on their way to the site of fertilization is centered on mitochondria. Additionally, they play a role in the apoptotic pathways, calcium regulation, redox balance, and flagellar movement—all of which are essential for gametic fusion, capacitation, acrosomal response, and flagellar movement (16,17). Therefore, a decline in any one of these various functions can frequently be connected to changes in sperm characteristics and fertility.

In this study, the adenine + cyclophosphamide was used to induce mice asthenozoospermia, and nine processed *Allium tuberosum Rottler* products were used to compare differences in efficacy for the treatment of asthenozoospermia in mice, and the most efficacious one will be analysed for changes in its chemical composition. Finally, we investigated the mechanism of *Allium tuberosum Rottler* for the treatment of asthenozoospermia in mice in terms of its modulation of mitochondrial autophagy. We present this article in accordance with the ARRIVE reporting checklist (available at https://tau.amegroups.com/article/view/10.21037/tau-24-274/rc).

Methods

Preparation of different Allium tuberosum Rottler artefacts and aqueous extract

In this experiment, six different *Allium tuberosum Rottler* artefacts were used in this experiment to compare their spermatogenic effects: raw *Allium tuberosum Rottler* (SP), stir-fried *Allium tuberosum Rottler* (CZP), stir-fried *Allium tuberosum Rottlers* with rice wine (JZP), stir-fried *Allium tuberosum Rottlers* with vinegar (KZP), and *Allium tuberosum Rottler* sauteed with salt and wine (GZP). The aforementioned *Allium tuberosum Rottlers* were made using the appropriate technique. Briefly, the raw *Allium tuberosum Rottler* was put in an iron pan and cooked over 500 ℃ until aromatic; after that, it was chilled to produce CZP. The JZP was made by placing the raw *Allium tuberosum Rottler* in an iron pot, adding the right amount of rice wine (10 kg for every 100 kg of Rottlers), heating, and then frying at 500 ℃ until the rice wine was sucked up by the Rottler. YZP: the raw *Allium tuberosum Rottlers* were placed in an iron kettle and appropriate amount of salt water (two kilograms of salt for every 100 kg of Rottler) was added. Once the salt water was absorbed by *Allium tuberosum Rottlers*, the mixture was heated and fried at 500 ℃ to obtain YZP. KZP: the raw *Allium tuberosum Rottlers* were put in the iron pot, and mixed with the right amount of vinegar (20 kg vinegar per 100 kg *Allium tuberosum Rottler*), when the vinegar was sucked by the *Allium tuberosum Rottlers*, the mixture was heated and fried with 500 ℃ to get KZP. GZP: the raw *Allium tuberosum Rottlers* were put in an iron pot, and mixed with the right amount of salt water and rice wine (2 kg salt and 10 kg rice wine per 100 kg *Allium tuberosum Rottler*), when the salt water and rice wine were absorbed by the *Allium tuberosum Rottler*, the mixture was heated and fried with 500 ℃ to get GZP.

Each of the above *Allium tuberosum Rottler* samples were weighed (50 g) respectively, then decocted with 10 times the amount and 8 times the amount of water for 1.5 hours. The water extracts were filtered and the filtrate were collected, then concentrated to 0.5 g/mL.

Reagents

Adenine and cyclophosphamide were purchased from platinum-strontium titanium technology Co., Ltd (Chongqing, China). Levocarnitine was obtained from Northeast Pharmaceutical Group Shenyang First Pharmaceutical Co., Ltd (Shenyang, China). Rabbit monoclonal antibodies PINK1 (ab186303), anti-LC3A/B (ab62721), anti-Parkin (ab315376), and anti-Caspase-3 (ab2302) were purchased from Abcam (Cambridge, UK). The Testosterone (S56K28Y04J), Follicle stimulating hormone Elisa Kit (Y89A29O71F) and prolactin Elisa Kit (P19L90E32C) ELISA kits were purchased from Beyotime Biotechnology Co., Ltd. (Shanghai, China). DCFH-DA and MitoSOX™ (BRED-036) were purchased from Boraid Bio-technology Co. (Shenzhen, China).

Animals

Specific Pathogen Free (SPF) grade male Kunming (KM) mice (weighing 20±2 g) were purchased from Army Medical University (Chongqing, China). During the experiment, the animals were housed individually in SPF facilities. Experiments were performed under a project license (No. ZMU21-2306-005) granted by Institutional Animal Ethics

Committee of Zunyi Medical University, in compliance with the Laboratory Animal Welfare and Ethics Committee of China.

The liquid chromatograph mass spectrometer (LC-MS) analysis

Various *Allium tuberosum Rottler* samples of 200 µL of aqueous decoction were added to 1,000 µL of 80% methanol solution and vortexed for 10 min. The sample was centrifuged for 10 min at 4 ℃ with a centrifugal force of 20,000 g, and the supernatant was filtered and analysed by LC-MS/MS (Waters ACQUITYTM UPLC HSST3).

Ion source: electrospray ionisation source (ESl); scanning mode: positive and negative ion switching scanning; detection mode: full mass/dd-MS2; resolution: 70,000 (full mass); 17,500 (dd-MS2); scanning range: 100.0–1,500.0 miz; Spary voltage: 3.8 Kv (positive); capillary temperature: 300 ℃; collision gas: high-purity argon (purity 29.809%); collision energy (N) CE: 30; sheath gas: nitrogen (purity 299.999%), 40 Arb; Aux gas heater temp: nitrogen (purity >99.999%), 350 ℃; data acquisition time: 30.0 min.

Chromatographic conditions: column: AQ-C18, 150 mm × 2.1 m, 1.8 µm (Wech). Flow rate: 0.30 mL/min; aqueous phase: 0.1% formic acid aqueous solution; organic phase: methanol; column temperature: 35 ℃; autosampler temperature: 10.0 ℃; injection volume: 5.00 µL.

Groups and treatments

Ninety male KM mice were randomly divided into nine groups according to body weight: Control, Model, Levocarnitine (LCT, 0.5 $g \cdot kg^{-1}$), SP (1 $g \cdot kg^{-1}$), CZP (1 $g \cdot kg^{-1}$), YZP (1 $g \cdot kg^{-1}$), JZP (1 $g \cdot kg^{-1}$), KZP (1 $g \cdot kg^{-1}$) and GZP (1 $g \cdot kg^{-1}$), 10 mice per group. Except for the normal group, the remaining mice were fed with adenine (7 d) and intraperitoneally injected with cyclophosphamide (30 $mg \cdot kg^{-1}$, 4 days) to make the asthenozoospermia model (18). Mice in the normal group were injected intraperitoneally with an equal volume of saline. After the asthenozoospermia model was established, mice in the LCT group were gavaged with 0.2 mL of levocanidin solution for 14 consecutive days. Mice in the different *Allium tuberosum Rottler* groups were gavaged with 0.2 mL of the corresponding aqueous extract of *Allium tuberosum Rottler* for 14 consecutive days, and mice in the normal and model groups were gavaged with an equal volume of saline for 14 consecutive days.

Testicular weight index

Mice in each experimental group were dislocated and executed, the abdominal cavity was opened, bilateral testes were removed, and the epididymal tissues on both sides were separated and weighed to calculate the weight index. Testicular weight index = total weight of bilateral testes/body weight × 100%.

Analysis of sperm parameters

The separated epididymal tissue was cut using ophthalmic scissors, allowed to stand for five minutes, and then pipetted and blown to homogenize it. It was then placed in a tiny flat dish with one milliliter of saline that had been heated to 37 ℃. To count the total number of sperm, the number of live sperm, the number of malformed sperm, and the number of sperm moving forward (number of sperm in class a + number of sperm in class b), a drop of the suspension was placed in a cell counting plate and immediately examined under a microscope. Class a sperm: indicates that sperm move forward in a fast and straight line, and in a straight line; class b sperm: indicates that sperm move forward in a slow or sluggish line, and in a slow motion; and to calculate the sperm activity rate, the sperm deformity rate, and sperm viability. Sperm viability = number of live spermatozoa/total number of spermatozoa ×100%; sperm abnormality rate = (number of spermatozoa with broken heads and tails)/total number of spermatozoa ×100%; and sperm viability = (number of spermatozoa of class a + number of spermatozoa of class b)/total number of spermatozoa ×100%.

Histological analysis

One side of mouse testis tissue was taken, fixed with animal testis tissue fixative, dehydrated with ethanol gradient, transparent with xylene, dipped in wax, paraffin sectioned, HE stained, dehydrated, transparent, sealed, and the pathological changes were observed under the microscope.

Elisa analysis

Following the weighing of the mice in each experimental group, blood was drawn from their orbits, centrifuged for 10 minutes at 4,000 rpm, and the supernatant was collected. The serum levels of T, PRL, and FSH were then determined in accordance with the ELISA kit's instructions.

Transmission electron microscope (TEM) detection

Mouse testicular tissues were fixed in 2.5% glutaraldehyde (4 ℃) for 4 h, rinsed three times in 0.1 mol/L phosphate buffer (pH 7.4) for 15 min each time, fixed in 1% osmium acid at room temperature (20 ℃) for 2 h, and rinsed three times in 0.1 mol/L phosphate buffer for 3 times, dehydrated in ethanol with different gradients, each time for 15 min, infiltrated with a 1:1 mixture of acetone: 812 embedding agent overnight, and then polymerised at 60 ℃. After 48 h, 60–80 nm ultrathin sections were made, and then double stained with uranium and lead (2% uranyl acetate saturated aqueous solution and lead citrate, each stained for 15 min). The sections were dried at room temperature overnight and observed by electron microscope (H-7650, HITACHI, Japan).

Western blot

The total protein of mice testicular tissue was extracted using RIPA lysate, and the total protein concentration was determined by BCA. The sample volume was 40 μg per well, separated by SDS-PAGE, and electrotransferred to PVDF membrane, and the membrane was closed with 5% skim milk powder solution for 2 h at room temperature, and primary antibodies β-actin (1:200), PINK1 (1:200), Light chain 3II (LC3-II)/Light chain 3I (LC3-I) (1:200), Parkin (1:200) and Caspase-3 (1:200) were added and incubated overnight at 4 ℃. Then the plus HRP-labelled goat anti-rabbit IgG (1:300) was then added and incubated for 2 h at room temperature. The gels were electrotransferred to nitrocellulose membranes using a Trans-turbo transfer system (Bio-Rad, USA).

Detection of mitochondrial membrane potential (ΔΨm) changes

ΔΨm was detected with the ΔΨm-dependent lipophilic dye JC-1. At JC-1 dye is a green fluorescent monomer at low mitochondrial membrane potential and generates red fluorescent aggregates at increased ΔΨm. Since JC-1 is ΔΨm sensitive, the amount of ΔΨm can be determined by measuring the ratio of red to green fluorescence. Mice testicular tissue cells were treated, and then they were incubated for 20 minutes at 37 ℃ with JC-1 staining solution (5 μg/mL). Afterward, the cells were twice washed with JC-1 staining buffer, and then they were examined under a fluorescence microscope. The fluorescence intensity of JC-1 monomer and JC-1 aggregates was determined using a multifunctional enzyme marker.

Immunofluorescence analysis

Mice testicular tissue cells were rinsed with PBS, fixed with 4% paraformaldehyde for 20 minutes at room temperature, and permeabilized for 10 minutes using Triton X-100 (T8200; Solarbio). After blocking the cells for 1 hour with immunostaining blocking buffer (Beyotime Biotechnology, P0252), they were treated with primary anti-LC3B (1: 200) and anti-TOM20 (1: 200) overnight at 4 ℃. After that, secondary goat anti-rabbit antibody (Solarbio, SE134; 1:1,000) were added and incubated at room temperature for 1 hour. Finally, the cells from each group were inspected with a fluorescent microscope (CKX53IPC; Olympus, Japan).

ROS detection

Cyto-ROS and Mito-ROS were detected using DCFH-DA and MitoSOX™, respectively, and intracellular ROS levels were measured using DCFH-DA staining, which is based on the fact that non-fluorescent DCFH-DA is converted to hyperfluorescent DCF when ROS are oxidised intracellularly, and the fluorescence intensity is directly proportional to the intracellular ROS levels. Mouse testicular tissue cells were loaded with DCFH-DA (1 μmol/L) at 37 ℃ for 15 min, and the green fluorescence intensity of DCFH-DA in each group was observed by fluorescence microscopy after 10 min. MitoSOX™ is an effective indicator for tracking superoxide in mitochondria of living cells with high selectivity. The mitochondrial mitochondria were treated with 0.5 μmol/L dose of MitoSOX™. The mitochondria were stained with 0.5 μmol/L dose of MitoSOX™ for 30 min in an incubator at 37 ℃, and the fluorescence intensity was observed by fluorescence microscope after treatment.

Statistical analysis

All data were analyzed using SPSS 19.0 Data were expressed as mean ± standard deviation (SD). For normally distributed values, a direct comparison between the two groups was conducted using an independent sample *t*-test. $P<0.05$.

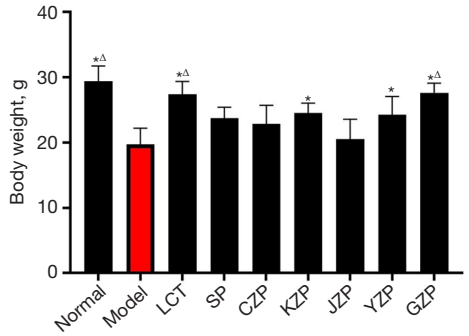

Figure 1 The body weight of mice in each group. Normal: mice were administered saline. Model, mice were administered saline; LCT, mice were administered levocarnitine; SP, mice were administered aqueous extract of raw *Allium tuberosum Rottlers*; CZP, mice were administered aqueous extract of stir-fried *Allium tuberosum Rottlers*; KZP, mice were administered aqueous extract of stir-fried *Allium tuberosum Rottlers* with vinegar; JZP, mice were administered aqueous extract of stir-fried *Allium tuberosum Rottlers* with rice wine; YZP, mice were administered aqueous extract of stir-fried *Allium tuberosum Rottlers* with salt; GZP, mice were administered aqueous extract of *Allium tuberosum Rottlers* sauteed with salt and rice wine. Statistical comparison of body weight indices of mice in each experimental group (*vs.* Model group, *P<0.05; *vs.* SP group, $^{\Delta}$P<0.05).

Table 1 Testicular weight index in each group

Group	n	Testicular weight index (%)
Normal	10	0.63±0.052*$^{\Delta}$
Model	9	0.53±0.065
LCT	8	0.58±0.033
SP	10	0.53±0.015
CZP	8	0.54±0.052
KZP	10	0.56±0.065
JZP	9	0.60±0.022*$^{\Delta}$
YZP	9	0.58±0.041
GZP	10	0.63±0.011*$^{\Delta}$

Data are presented as mean ± standard deviation. Normal: mice were administered saline. Model, mice were administered saline; LCT, mice were administered levocarnitine; SP, mice were administered aqueous extract of raw *Allium tuberosum Rottlers*; CZP, mice were administered aqueous extract of stir-fried *Allium tuberosum Rottlers*; YZP, mice were administered aqueous extract of stir-fried *Allium tuberosum Rottlers* with salt; JZP, mice were administered aqueous extract of stir-fried *Allium tuberosum Rottlers* with rice wine; KZP, mice were administered aqueous extract of stir-fried *Allium tuberosum Rottlers* with vinegar; GZP, mice were administered aqueous extract of *Allium tuberosum Rottlers* sauteed with salt and rice wine. *vs.* Model group, *P<0.05; *vs.* SP group, $^{\Delta}$P<0.05.

Results

Changes of body weight of mice in each group

As shown in *Figure 1*, there was a significant reduction (P<0.05) in body weight of mice in the model group compared with the normal group. Compared with the model group, the weight of mice in the LCT group, KZP group, YZP group, and GZP group increased significantly (P<0.05). The rest of the groups were not statistically significant (P>0.05) compared with the model group. Meanwhile, compared with the SP group, the weight of mice in the LCT group and GZP group increased significantly (P<0.05).

Changes of testicular weight index in each group

As shown in *Table 1*, there was a significant reduction (P=0.02) in testicular weight index of mice in the model group compared with the normal group. Compared with the model group, the testicular weight index of mice in the JZP group and GZP group increased significantly (P=0.03). The rest of the groups were not statistically significant (P>0.05) compared with the model group. Meanwhile, compared with the SP group, the testicular weight index of mice in the JZP group and GZP group increased significantly (P<0.05).

Total sperm count, sperm viability, sperm abnormality rate and sperm viability in each group of mice

Compared with the normal group, the total number of spermatozoa in the model group was extremely significantly lower (P=0.001). Compared with the model group, the total number of spermatozoa in the LCT group and GZP group were extremely significantly higher (P=0.009), and the total number of spermatozoa in the KZP group and JZP group were significantly higher (P=0.04). Compared with the normal group, the sperm viability of mice in the model group was highly significantly reduced (P=0.003). Compared with the model group, the sperm viability of mice in the LCT group and GZP group were extremely significantly higher (P=0.005), and the sperm viability of mice in the KZP group and JZP group were significantly higher (P=0.03). Compared with the normal group, the sperm abnormality rate of mice in the model group was

Table 2 Total sperm count, sperm viability, sperm abnormality rate and sperm motility of mice in various groups

Group	Total number of spermatozoa (×10^6/mL)	Sperm viability rate (%)	Sperm abnormality rate (%)	Sperm motility rate (%)
Normal	120.58±15.65**	80.21±7.29**	9.83±1.28**	70.38±6.21**
Model	78.49±9.57	36.28±5.37	43.29±5.73	48.49±5.09
LCT	116.35±13.76**$^{\Delta}$	73.19±6.41**$^{\Delta}$	17.41±3.86**$^{\Delta}$	61.29±4.98**$^{\Delta}$
SP	82.36±11.40	38.29±4.53	36.28±5.31	42.89±3.76
CZP	77.48±9.41	41.23±5.02	32.49±4.22*	50.42±6.10
KZP	87.34±13.62*	45.87±3.98*	34.59±4.03*	57.23±4.79*
JZP	91.62±10.45*	57.43±8.79*	30.29±6.21*	58.32±4.81*
YZP	86.49±7.54	39.66±6.13	41.29±5.49	41.83±6.02
GZP	104.34±9.67**$^{\Delta}$	70.58±6.69**$^{\Delta}$	21.43±5.18**$^{\Delta}$	62.48±5.34**$^{\Delta}$

Data are presented as mean ± standard deviation. Normal: mice were administered saline. Model, mice were administered saline; LCT, mice were administered levocarnitine; SP, mice were administered aqueous extract of raw *Allium tuberosum Rottlers*; CZP, mice were administered aqueous extract of stir-fried *Allium tuberosum Rottlers*; YZP, mice were administered aqueous extract of stir-fried *Allium tuberosum Rottlers* with salt; JZP, mice were administered aqueous extract of stir-fried *Allium tuberosum Rottlers* with rice wine; KZP, mice were administered aqueous extract of stir-fried *Allium tuberosum Rottlers* with vinegar; GZP, mice were administered aqueous extract of *Allium tuberosum Rottlers* sauteed with salt and rice wine. *vs.* Model group, *P<0.05, **P<0.01; *vs.* SP group, $^{\Delta}$P<0.05.

highly significantly higher (P=0.004). Compared with the model group, the sperm abnormality rate of mice in the LCT group and GZP group were extremely significantly lower (P=0.001). And the sperm abnormality rate of mice in the CZP, KZP, and JZP groups was significantly lower (P=0.02). Compared with the normal group, the sperm motility of mice in the model group was highly significantly reduced (P=0.001). Compared with the model group, the sperm viability of mice in the LCT group and GZP group were extremely significantly higher (P=0.004). The sperm viability of mice in the KZP and JZP groups was significantly elevated (P=0.02). Meanwhile, compared with the SP group, the total number of spermatozoa, sperm viability, and sperm motility of mice in the GZP group increased significantly (P=0.04), while the sperm abnormality decreased significantly (P=0.03), suggesting the spermatogenic effect of *Allium tuberosum Rottler* can be enhanced by processing it with rice wine and salt. The results are shown in *Table 2*.

Histopathological morphology of testis in various groups of mice

Histopathological results of the testes of mice in each group showed that the spermatogenic cells in the testes of mice in the normal group were arranged in a hierarchical manner and occupied a large area, with abundant spermatogenic cells at all levels, and cells at all levels in the process of spermatogenesis were easy to be seen, and a large number of sperm could be seen in the lumen of the ducts. Compared with the normal group, the spermatogenic epithelium of the testes in the model group was thinned, the spermatogenic cells were loosely arranged and disorganized (shown by red arrows), the cells at all levels of spermatogenesis were damaged and differentiated abnormally (shown by black arrows), and a small number of spermatozoa were seen in the lumen of the tubes or no spermatozoa were seen. Compared with the model group, the spermatogenic epithelium of the testicular tissue of mice in the LCT group, YZP group, JZP group, and GZP group showed that the degree of spermatogenic disorders had been effectively alleviated, the spermatogenic cell layer was thickened, and cells at all levels in the process of spermatogenesis were seen in greater numbers, the spermatogonial differentiation and formation process had been significantly improved, and the total number of spermatids in the lumen had been increased. There was no significant change in the rest groups compared with the model group. The results of testicular pathomorphological tests in all groups of mice once again demonstrated that the spermatogenic effect of *Allium tuberosum Rottler* can be enhanced by processing it with rice wine and salt. The results are shown in *Figure 2*.

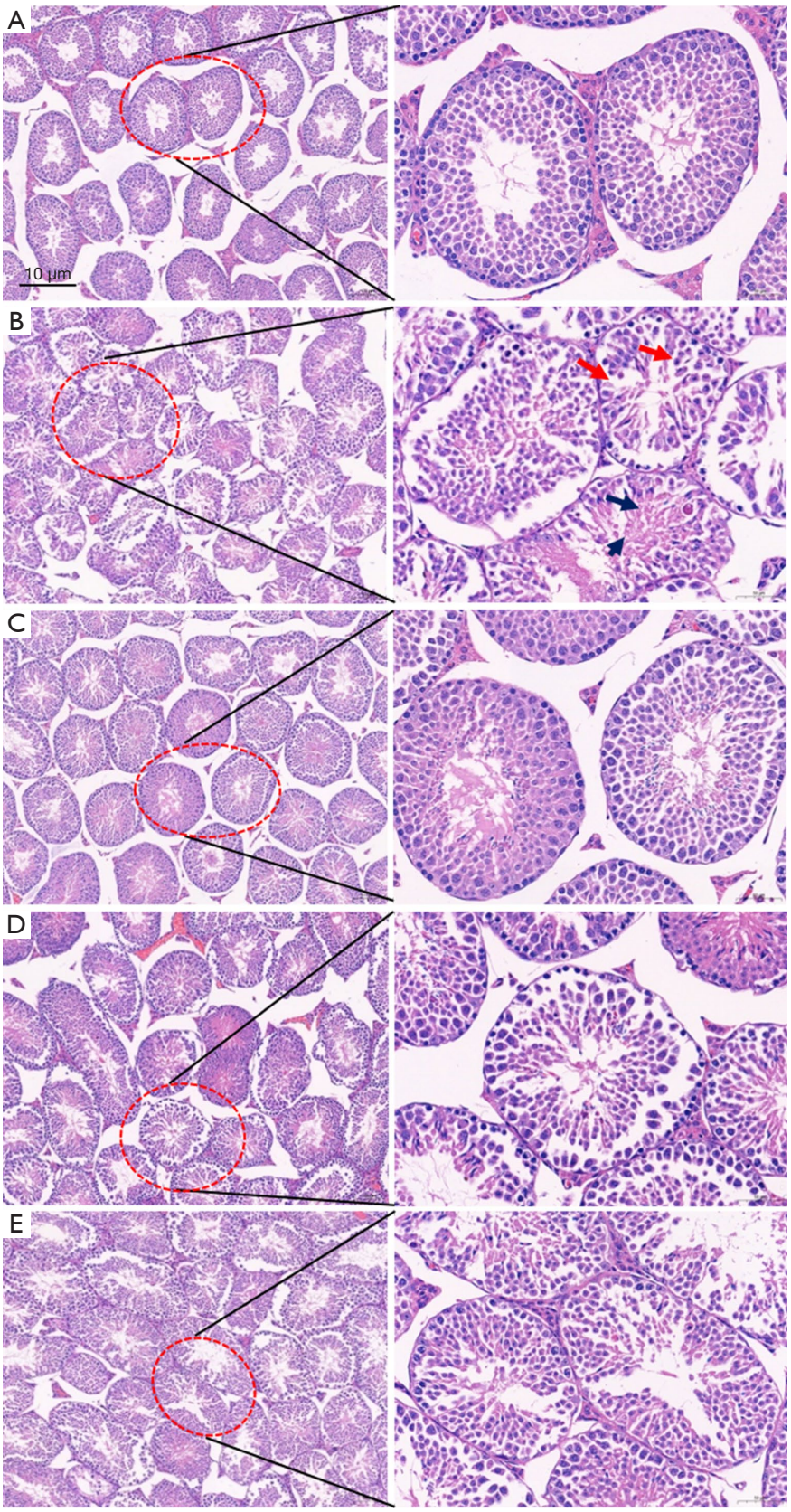

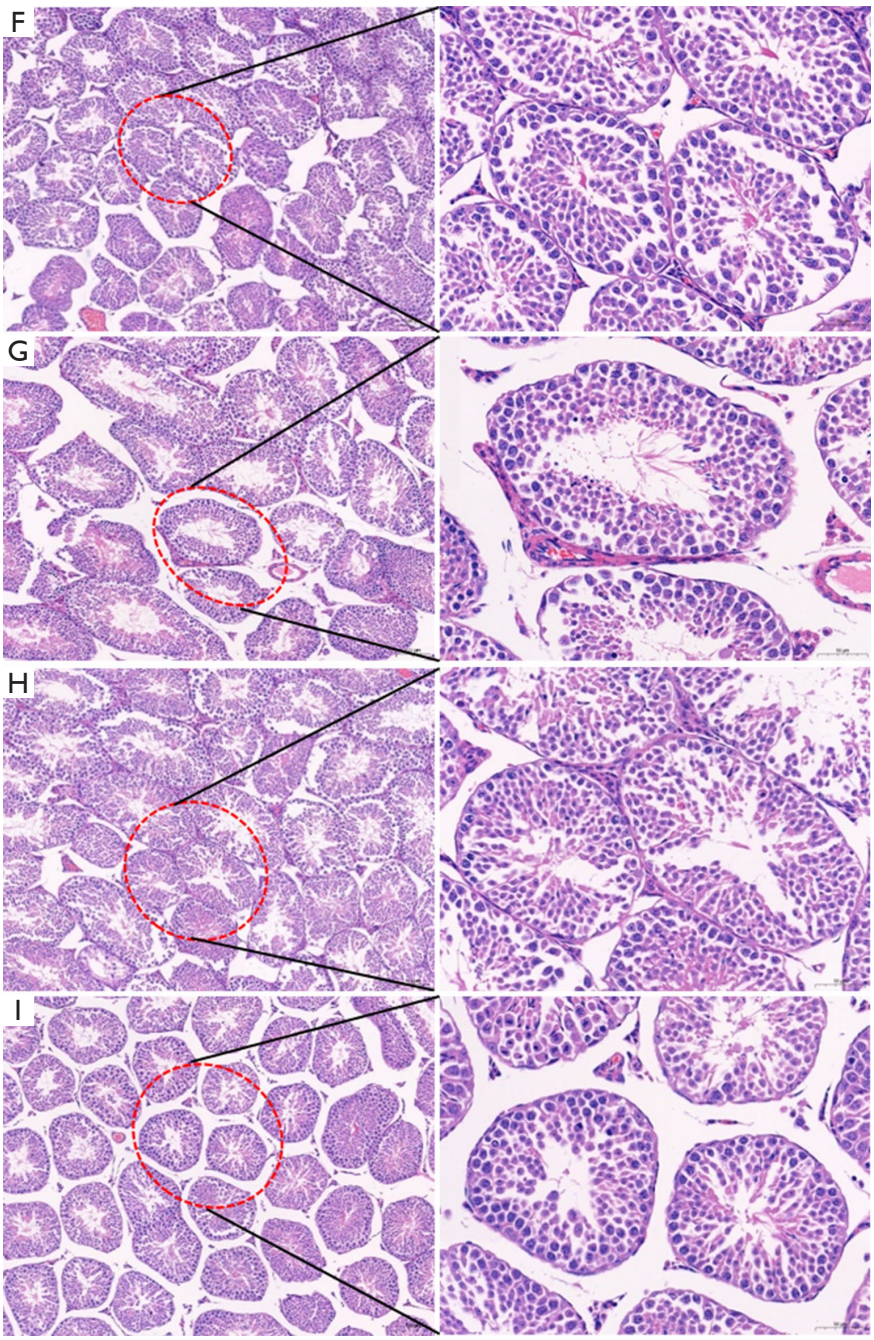

Figure 2 H&E stained testis sections showing pathological morphology of each group. (A) Normal: mice were administered saline. (B) Model: mice were administered saline. (C) LCT: mice were administered levocarnitine. (D) SP: mice were administered aqueous extract of raw *Allium tuberosum Rottlers*. (E) CZP: mice were administered aqueous extract of stir-fried *Allium tuberosum Rottlers*. (F) YZP: mice were administered aqueous extract of stir-fried *Allium tuberosum Rottlers* with salt. (G) JZP: mice were administered aqueous extract of stir-fried *Allium tuberosum Rottlers* with rice wine. (H) KZP: mice were administered aqueous extract of stir-fried *Allium tuberosum Rottlers* with vinegar. (I) GZP: mice were administered aqueous extract of *Allium tuberosum Rottlers* sauteed with salt and rice wine. The red arrows indicate the spermatogenic epithelium of the testes in the model group was thinned, the spermatogenic cells were loosely arranged and disorganized. The black arrows indicate the cells at all levels of spermatogenesis were damaged and differentiated abnormally.

Table 3 Serum T, FSH and PRL levels of mice in each group

Group	T (pg/mL)	PRL (ng/mL)	FSH (ng/mL)
Normal	187.38±11.06*	8.23±1.16*	24.53±4.19*
Model	112.41±13.28	6.49±1.32	13.98±3.55
LCT	146.98±8.26*	6.18±0.31	19.64±6.21*
SP	129.67±25.81	6.54±1.02	12.85±2.79
CZP	132.68±14.37	6.79±0.61	13.09±3.31
YZP	139.32±10.26*	6.42±0.43	15.29±3.92
JZP	126.46±9.31	6.92±0.71	16.43±4.03
KZP	131.22±16.82	6.43±0.52	14.59±6.22
GZP	137.38±8.26*	7.02±0.41*	18.39±5.81*

Data are presented as mean ± standard deviation. Normal: mice were administered saline. Model, mice were administered saline; LCT, mice were administered levocarnitine; SP, mice were administered aqueous extract of raw *Allium tuberosum Rottlers*; CZP, mice were administered aqueous extract of stir-fried *Allium tuberosum Rottlers*; YZP, mice were administered aqueous extract of stir-fried *Allium tuberosum Rottlers* with salt; JZP, mice were administered aqueous extract of stir-fried *Allium tuberosum Rottlers* with rice wine; KZP, mice were administered aqueous extract of stir-fried *Allium tuberosum Rottlers* with vinegar; GZP, mice were administered aqueous extract of *Allium tuberosum Rottlers* sauteed with salt and rice wine. *vs.* Model group, *P<0.05.

Serum sex hormone levels of mice in each group

Compared with the normal group, the serum T, FSH and PRL levels of mice in the model group were significantly decreased (P=0.04); compared with the model group, the serum T and FSH levels of mice in the LCT group were significantly increased (P=0.02), and there was no significant change in the PRL level. Compared with the model group, the serum T levels of mice in YZP and GZP groups were significantly elevated (P=0.03), and the serum FSH levels of mice in GZP group were significantly elevated (P=0.02). There were no significant changes in serum T and FSH levels in the remaining concoction groups. Compared with the model group, the serum PRL levels of mice in the GZP group were significantly elevated (P=0.02), and there was no significant change in the serum PRL levels of mice in the rest of the groups compared with the model group. The results are shown in *Table 3*.

Chemical composition change analysis

We screened GZP to exhibit the best therapeutic effect on asthenozoospermia in mice through pharmacodynamic experiments, and further, we compared the chemical compositional differences between SP and GZP using LC-MS/MS. The total ion flow diagram for LC-MS/MS detection is shown in *Figure 3A*, and the positive and negative ion flow diagrams are shown in *Figure 3B* and *Figure 3C*, respectively.

Compared with the SP, a total of 1,032 compounds were changed in GZP, of which 331 compounds were increased and 701 compounds were decreased. Based on the differential compound screening conditions of VIP ≥1 and P value ≤0.05, we screened the top 10 compounds with decreasing levels and the top 10 compounds with increasing levels respectively, as shown in *Figure 4* and *Table 4*. Of these 10 compounds with elevated levels, (S)-3-(Allylsulphinyl)-L-alanine, also known as Allicin (*Figure 5*), showed the most significant increase in content, which may be one of the active ingredients in GZP for the treatment of asthenozoospermia in mice.

Study on the mechanism of GZP in the treatment of asthenospermia in mice

Forty male KM mice were randomly divided into four groups: Control, Model, Levocarnitine (LCT, 0.5g·kg^{-1}) and GZP (1g·kg^{-1}), 10 mice per group. Except for the normal group, the remaining mice were fed with adenine (7 d) and intraperitoneally injected with cyclophosphamide (30 mg·kg^{-1}, 4 days) to make the asthenozoospermia model. Mice in the normal group were injected intraperitoneally with an equal volume of saline. After the asthenozoospermia model was established, mice in the LCT group and GZP group were gavaged with 0.2 mL of levocanidin or aqueous extract solution of *Allium tuberosum Rottlers* 14 consecutive days, and mice in the normal and model groups were gavaged with an equal volume of saline for 14 consecutive days. At 14th day, both testicles of mice in each experimental group were taken out for detection.

ΔΨm changes of mice testicular tissue

As shown in *Figure 6*, compared with the normal group, the ΔΨm of mice testicular tissue in the model group was extremely significantly lower (P=0.002); compared with the model group, the ΔΨm of mice testicular tissue in the LCT group and GZP group were extremely significantly higher (P=0.005).

ROS detection

As shown in *Figure 7*, compared with the normal group,

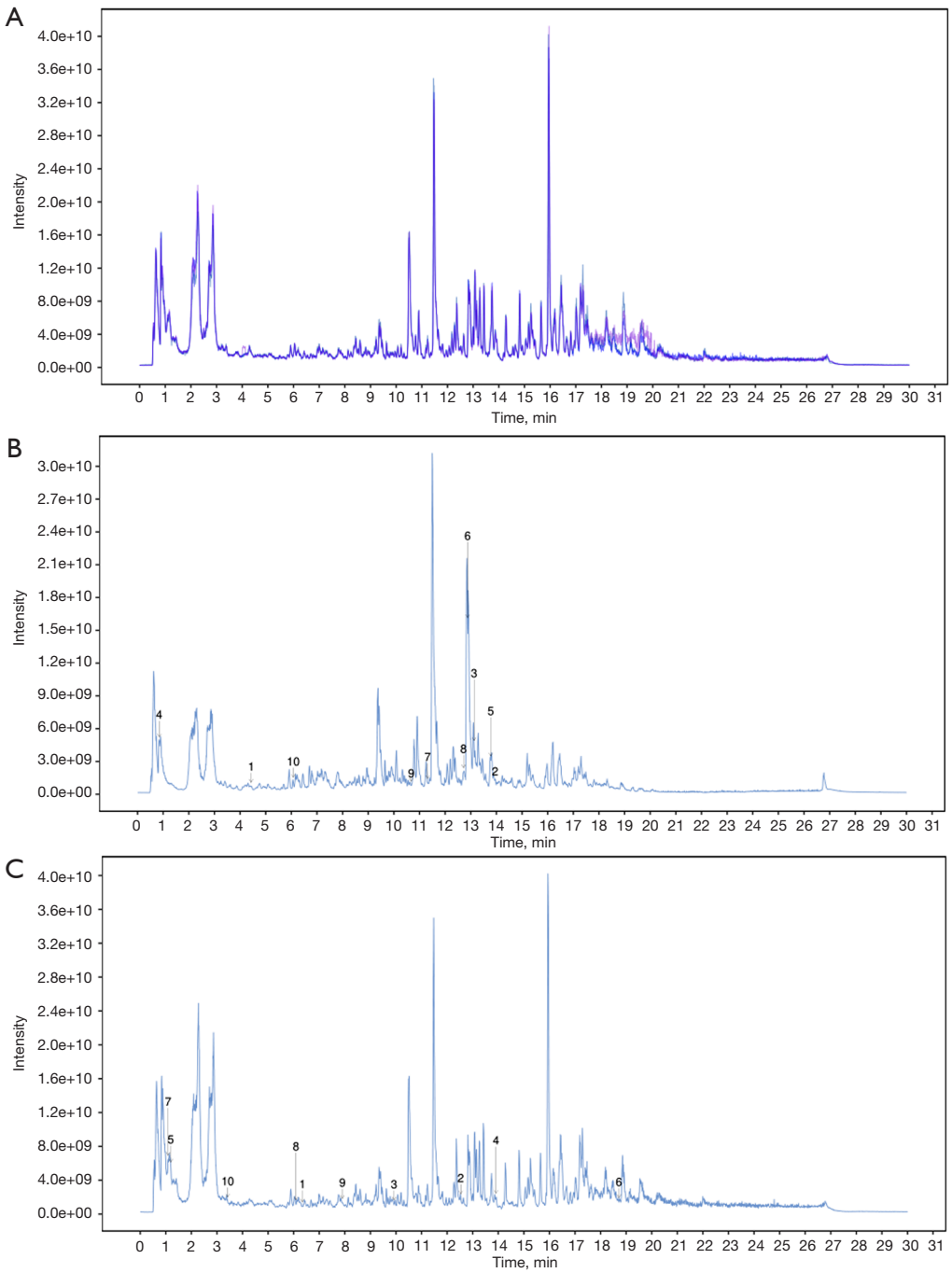

Figure 3 Ion flow diagram of GZP detected by LC-MS/MS. (A) The total ion flow diagram. (B) The positive ion flow diagrams (1. Kudzusaponin SA4; 2. 2-Linoleoyl Glycerol; 3. (2S,3R,4R,5R,6S)-2-[(2R,3R,4S,5R,6R)-2-[2-(3,4-dihydroxyphenyl)ethoxy]-3,5-dihydroxy-6-(hydroxymethyl)oxan-4-yl]oxy-6-methyloxane-3,4,5-triol; 4. Dicyclopenta[a,i]phenanthrene-3a(1H)-carboxylic acid,10-formyloctadecahydro-9-hydroxy-5a,5b,8,8,10a-pentamethyl-1-(1-methylethenyl); 5. 14-Deoxyandrographolide; 6. (S)-3-(Allylsulphinyl)-L-alanine; 7. DL-Homocysteine; 8. (1S,2R,5R,6R,10R,13S,15S)-5-[(2R,3E,5R)-5,6-dimethylhept-3-en-2-yl]-6,10-dimethyl-16,17-dioxapentacyclo[13.2.2.$0^{1,9}$.$0^{2,6}$.$0^{10,15}$]nonadec-18-en-13-ol; 9. S-Furanopetasitin; 10. Corchorifatty acid D). (C) The negative ion flow diagrams (1. 3-propan-2-yl-2,3,6,7,8,8a-hexahydropyrrolo[1,2-a]pyrazine-1,4-dione; 2. 3,5-Didecanoylpyridine; 3. Pyroglutamic acid; 4. 7-Isothiocyanato-1-heptene; 5. Pyridoxine; 6. Tyramine; 7. 3-Methyl-2-butene-1-thiol; 8. Furostane base -1H2O + 1O, O-Hex, O-Hex-Hex; 9. Cyclo(leucylprolyl); 10. 2-Ethyl-6-methylpyrazine).

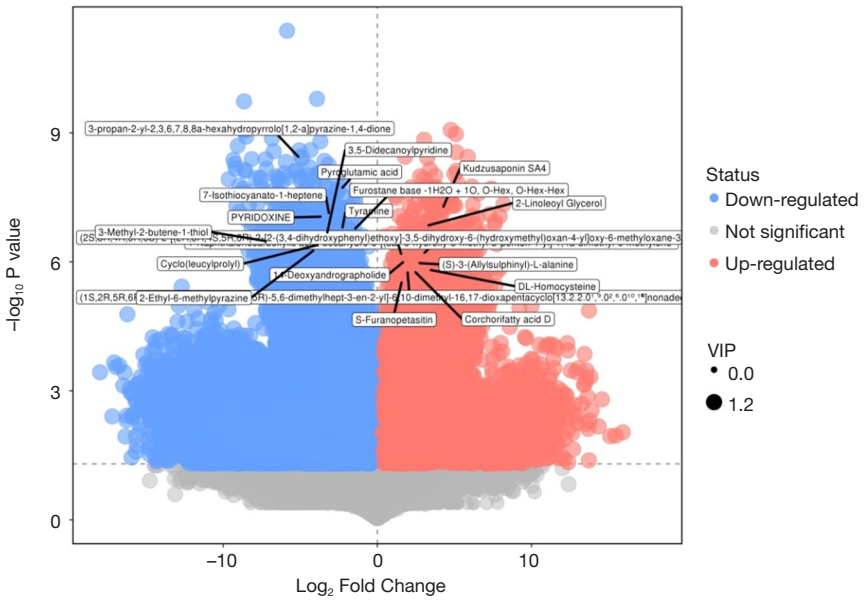

Figure 4 Volcano plots of the top 10 compounds with the most significant changes in content.

Table 4 Top 10 compounds with the most significant changes in content

No.	Compounds	
	Up-regulated	Down-regulated
1	Kudzusaponin SA4	3-propan-2-yl-2,3,6,7,8,8a-hexahydropyrrolo[1,2-a]pyrazine-1,4-dione
2	2-Linoleoyl Glycerol	3,5-Didecanoylpyridine
3	(2S,3R,4R,5R,6S)-2-[(2R,3R,4S,5R,6R)-2-[2-(3,4-dihydroxyphenyl)ethoxy]-3,5-dihydroxy-6-(hydroxymethyl)oxan-4-yl]oxy-6-methyloxane-3,4,5-triol	Pyroglutamic acid
4	Dicyclopenta[a,i]phenanthrene-3a(1H)-carboxylic acid, 10-formyloctadecahydro-9-hydroxy-5a,5b,8,8,10a-pentamethyl-1-(1-methylethenyl)	7-Isothiocyanato-1-heptene
5	14-Deoxyandrographolide	Pyridoxine
6	(S)-3-(Allylsulphinyl)-L-alanine	Tyramine
7	DL-Homocysteine	3-Methyl-2-butene-1-thiol
8	(1S,2R,5R,6R,10R,13S,15S)-5-[(2R,3E,5R)-5,6-dimethylhept-3-en-2-yl]-6,10-dimethyl-16,17-dioxapentacyclo[13.2.2.0^{1},^{9}.0^{2},^{6}.0^{10},^{15}]nonadec-18-en-13-ol	Furostane base -1H2O + 1O, O-Hex, O-Hex-Hex
9	S-Furanopetasitin	Cyclo(leucylprolyl)
10	Corchorifatty acid D	2-Ethyl-6-methylpyrazine

the Cyto-ROS and Mito-ROS levels were significantly increased in the testicular tissue cells of mice in the model group (P=0.003); compared with the model group, both of the Cyto-ROS and Mito-ROS levels were significantly decreased in the testicular tissue cells of mice in the LCT group and GZP group (P=0.001), suggesting that GZP scavenges excessive ROS in the testicular histiocytic cells of mice with asthenozoospermia.

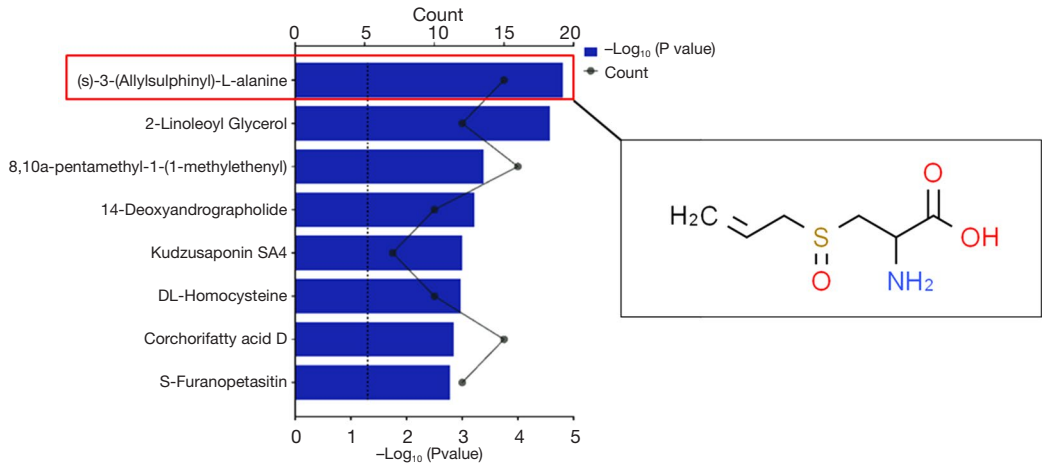

Figure 5 Changes in the content of (S)-3-(Allylsulphinyl)-L-alanine(Allicin) and its chemical structure.

TEM detection of mitochondrial morphology in testicular tissue

TEM observation of mitochondria in mice testis cells showed that the mitochondrial structure of testis cells of mice in the normal group was intact, the morphology of the mitochondrial membrane and cristae was normal, and there were scarcely any autophagosomes formed in the mitochondria with obvious double-layered membranes, as shown in *Figure 8A*. In contrast, the mitochondrial structure in the testicular cells of mice in the model group was obviously damaged, the mitochondrial membrane was disrupted and disintegrated, the mitochondrial cristae were swollen, broken, or even disappeared, and there were many autophagosomes in the mitochondria, as shown in *Figure 8B*. Compared with the model group, mitochondrial damage in mouse testicular cells in the GZP and LCT treatment groups was significantly reduced, and the number of autophagosomes was significantly decreased, as shown in *Figure 8C* and *Figure 8D*, respectively. Further co-localization of LC3 and mitochondria by immunofluorescence revealed that LC3 fluorescence intensity in mitochondria of testicular cells of mice in the model group was significantly enhanced compared with that of the normal group (*Figure 8E*), demonstrating that mitophagy was over-activated. While the LC3 fluorescence intensity in the mitochondria of testicular cells in the GZP-treated group was significantly weaker than that in the model group, suggesting that mitophagy was inhibited.

Expression of mitochondrial autophagy related proteins

As shown in *Figure 9*, compared with the normal group, the expression levels of PINK1, Parkin, LC3-I/LC3-II, and Caspase-3 protein were significantly increased in the testicular tissue cells of mice in the model group (P=0.005), indicating that mitochondrial autophagy was overactivated and apoptosis was triggered in the testicular tissue cells of mice in the model group. Compared with the model group, the expression levels of PINK1, Parkin, LC3-I/LC3-II, and Caspase-3 protein were significantly decreased in the testicular tissue cells of mice in the LCT group and GZP group (P=0.003), suggesting that GZP inhibits excessive mitochondrial autophagy and apoptosis in testicular histiocytes of mice with asthenozoospermia.

Discussion

In this study, we established a recognized mouse model of asthenozoospermia using oral adenine and intraperitoneal injection of cyclophosphamide and screened six commonly used processed *Allium tuberosum Rottler* for pharmacodynamic effects. Cyclophosphamide, a commonly used antitumor drug and immunosuppressant, is reproductively toxic and can damage spermatogonial stem cells, affecting pathways such as p53 and Fas/FasL, thereby inducing germ cell malformations, mutations in genetic material, and apoptosis (19). Studies have shown that cyclophosphamide can cause azoospermia or oligospermia, leading to infertility or malformations (6). We combined all the pharmacodynamic evaluation indexes and concluded that GZP showed the best therapeutic effect in improving the total number of spermatozoa, sperm survival rate, sperm viability, and sperm deformity rate in mice, indicating

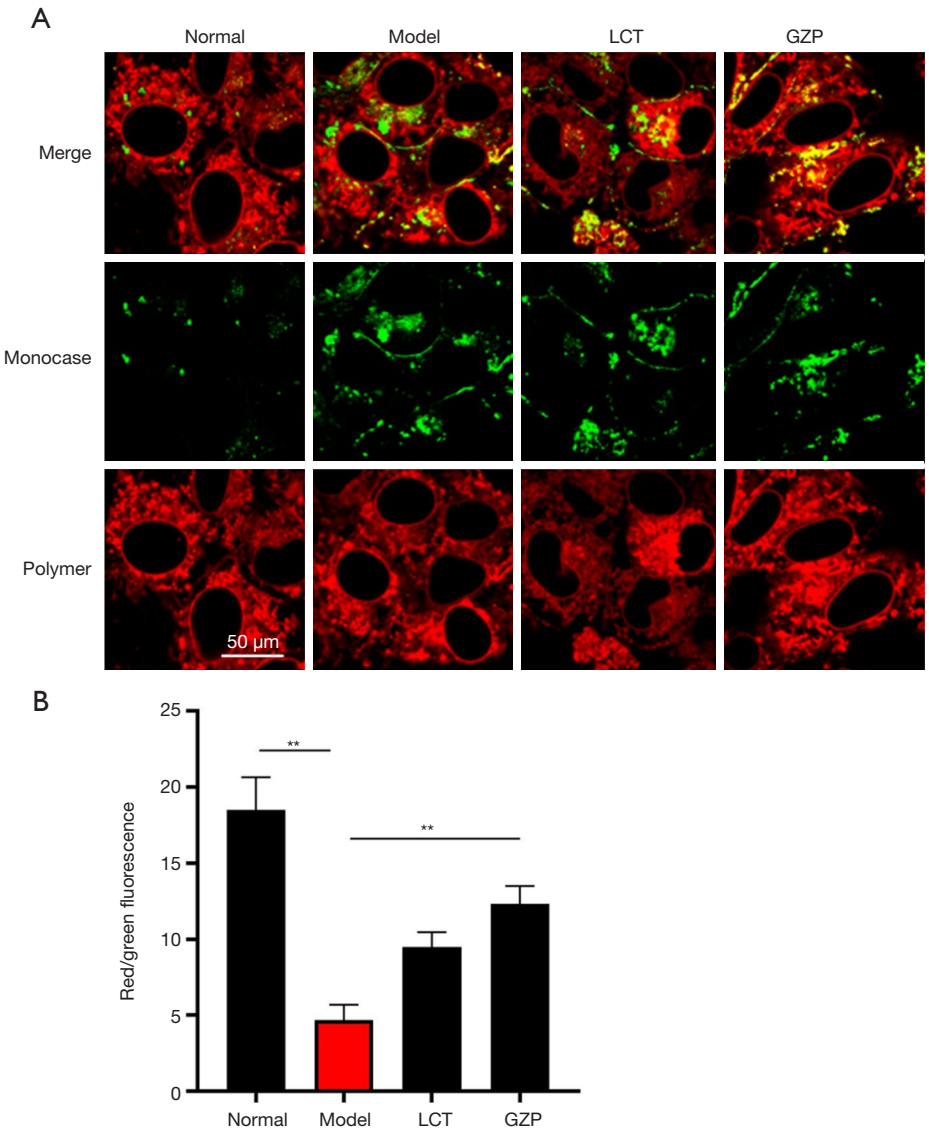

Figure 6 Effect of GZP on ΔΨm of testicular tissue cells in mice with asthenospermia. (A) ΔΨm was detected with the ΔΨm-dependent lipophilic dye JC-1. (B) Statistical comparison of ΔΨm of mice in each experimental group (*vs.* Model group, **P<0.01). LCT, mice were administered levocarnitine; GZP, mice were administered aqueous extract of *Allium tuberosum Rottlers* sauteed with salt and rice wine.

that GZP could promote spermatogenesis and enhance sperm quality in mice. Meanwhile, compared with the model group, GZP alleviated the abnormal pathological morphology of mouse testis, for example, alleviating the degree of spermatogenic disorders, thickening the spermatogenic cell layer, improving the spermatogonial differentiation and formation process, and increasing the total number of spermatids in the lumen. This indicated that the spermatogenic disorders in the testicular tissues of mice were effectively modified after GZP treatment.

The T is an important component of androgens, and its level is closely related to the spermatogenic function of the testis, which promotes spermatogenesis and maturation and enhances the quantity and quality of spermatozoa. FSH acts on the supportive cells to secrete T, and PRL, although not considered a "classical" sex hormone, may play a role in male endocrine control. The results showed that serum T, FSH, and PRL levels in the model group were significantly lower than those in the normal group, and the serum sex hormone levels in the mice were increased after treatment

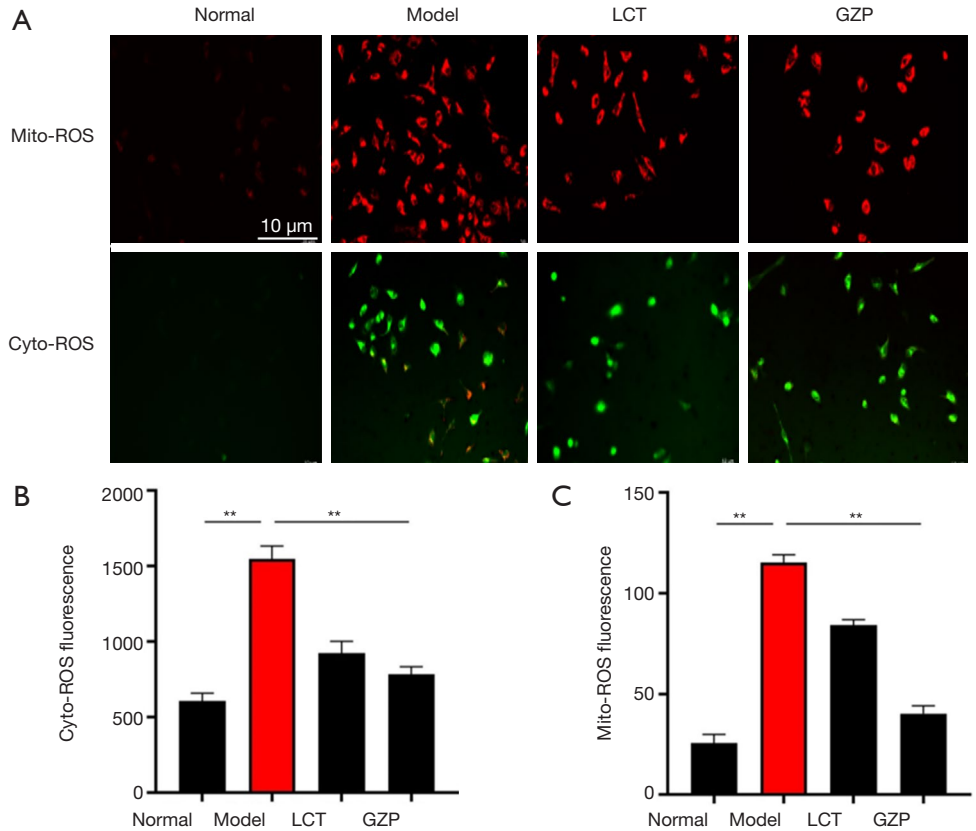

Figure 7 Effect of GZP on ROS level of testicular tissue cells in mice with asthenospermia. (A) Cyto-ROS and Mito-ROS were detected using DCFH-DA and MitoSOX™, respectively. (B) Statistical comparison of Cyto-ROS of mice in each experimental group (*vs.* Model group, **P<0.01). (C) Statistical comparison of Mito-ROS of mice in each experimental group (*vs.* Model group, **P<0.01). LCT, mice were administered Levocarnitine; GZP, mice were administered aqueous extract of *Allium tuberosum Rottlers* sauteed with salt and rice wine.

with GZP, suggesting that GZP can improve spermatogenic disorders in mice with oligozoospermia by increasing serum sex hormone levels. In conclusion, we believe that GZP exhibits optimal therapeutic effects on asthenozoospermia in mice.

Based on this, we compared the variations in chemical composition between SP and GZP using LC-MS. In GZP, we discovered that a total of 1032 compounds were altered, of which 331 had an increase and 701 had a drop. We removed the top 10 compounds with levels that were declining and the top 10 compounds that were increasing. We also discovered that allicin had the biggest content rise. According to Nadeem *et al.* (20), allicin is an amino acid that contains sulfur and has pharmacological properties that include scavenging free radicals, anti-tumor, anti-thrombotic, and hypolipidemic effects. According to Shi *et al.* (21), allicin has a potent antioxidant effect and can lower MDA, TC, and LDL-C levels while raising SOD activity and HDL-C levels in hyperlipidemic mice. In addition, Allicin can significantly reduce the adhesion of monocytes and endothelial cells, inhibit TNF-α-induced vascular cell adhesion molecule VCAM-1 expression; inhibit the increase of cellular superoxide anion products and NADH oxidase subunit NOX4 up-regulation; and at the same time, inhibit the attenuation of the cellular mitochondrial membrane potential, which has a good control of TNF-α-mediated inflammatory injury and cardiovascular disease (22).

In recent years, a large number of studies have shown that oxidative stress triggered by increased ROS is an important factor affecting sperm quality in men (23). Oxidative stress is caused by an imbalance between reactive oxygen radicals and the antioxidant system and is considered to be one of the main causes of male infertility, sperm

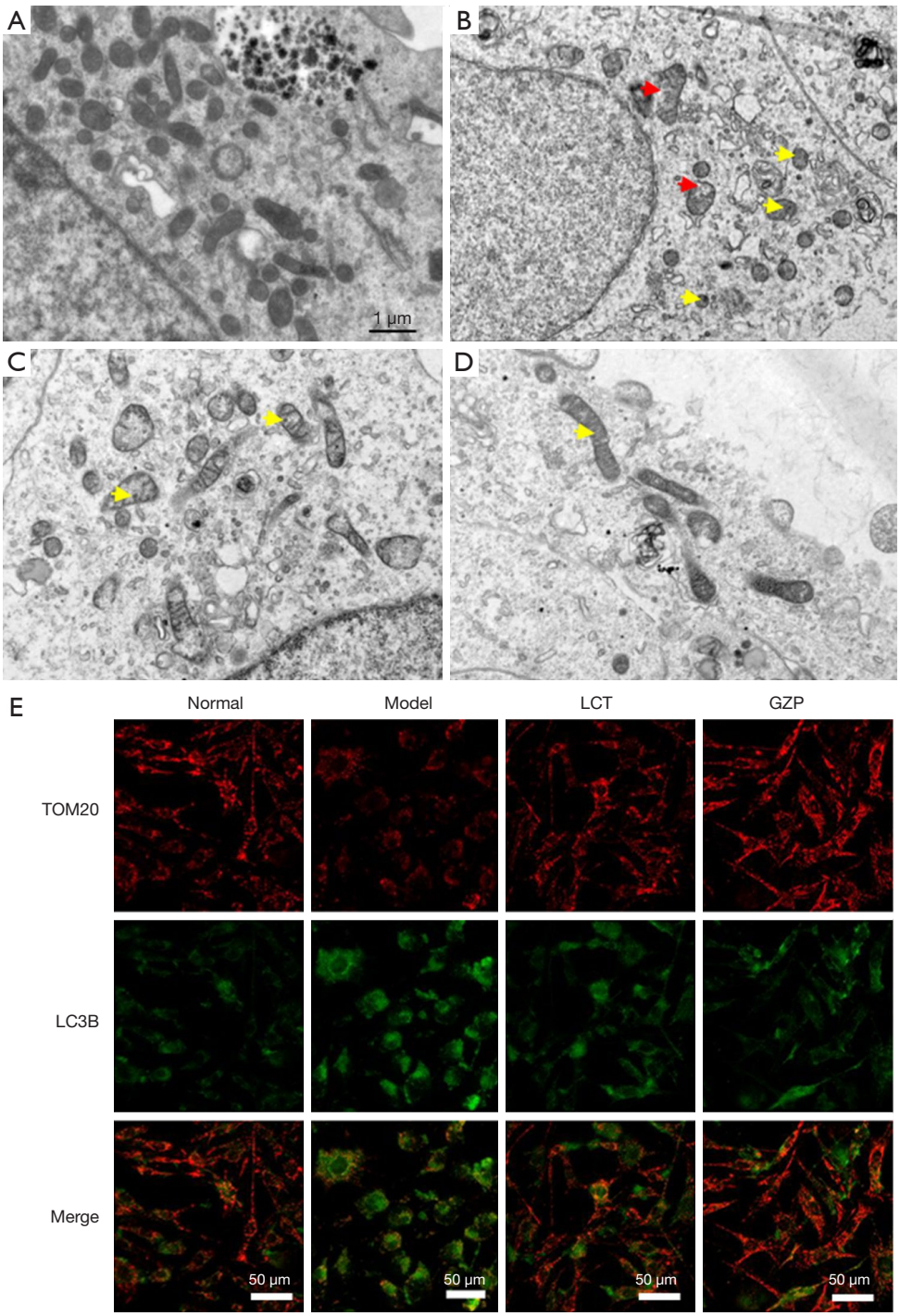

Figure 8 Transmission electron microscopy images of mitochondria and autophagosomes in mice testis cells. (A) Normal: mice were administered saline. (B) Model: mice were administered saline. (C) LCT: mice were administered Levocarnitine. (D) GZP: mice were administered aqueous extract of *Allium tuberosum Rottlers* sauteed with salt and rice wine. (E) Co-localization of mitochondria and LC3 in mouse testicular tissue cells. The broken mitochondria are marked by red arrowheads. The autophagosomes are marked with yellow arrowheads. LCT, mice were administered levocarnitine; GZP, mice were administered aqueous extract of *Allium tuberosum Rottlers* sauteed with salt and rice wine.

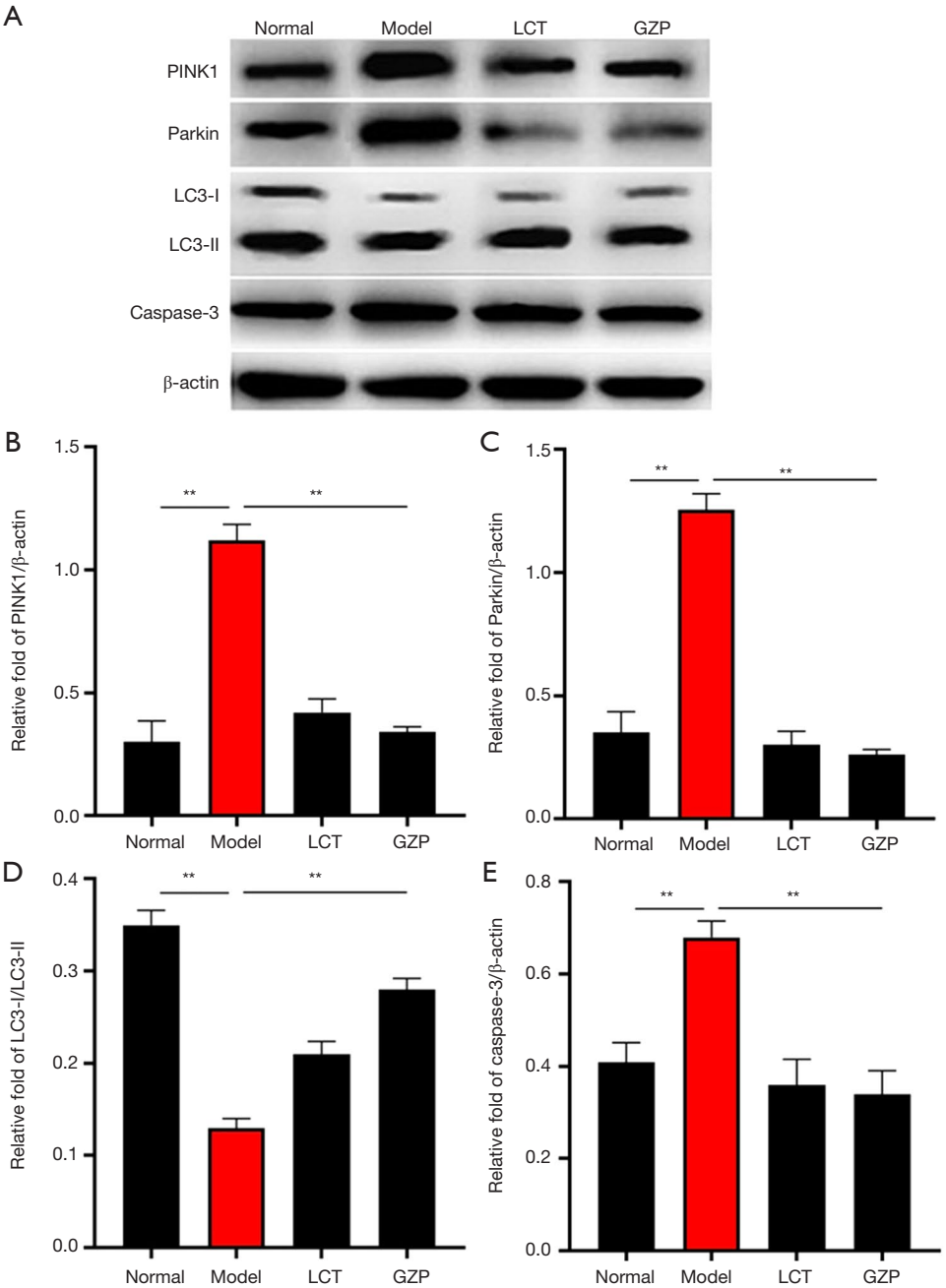

Figure 9 GZP inhibits mitochondrial autophagy and apoptosis in testicular histiocytes of mice with asthenozoospermia. (A) Relative protein levels of PINK1, Parkin, LC3-I/II and Caspase-3 were detected by western blotting. (B-E) Statistical comparison of PINK1, Parkin, LC3-I/II and Caspase-3 of mice in each experimental group. Data were expressed after being normalized to β-actin (*vs.* Model group, **P<0.01). LCT, mice were administered levocarnitine; GZP, mice were administered aqueous extract of *Allium tuberosum Rottlers* sauteed with salt and rice wine.

DNA fragmentation, and abnormal semen parameters (24). Oxidative stress damages DNA in the nucleus and mitochondria and leads to lipid peroxidation in sperm cells, resulting in sperm DNA fragmentation with loss of genetic material, triggering abnormal apoptosis of sperm cells and decreased sperm viability (25). Ultimately, this leads to the increase of weak and fragmented spermatozoa, resulting in the decrease of male fertility or infertility. GZP has a significant therapeutic effect on weak spermatozoa in mice, and the content of Allicin in GZP is significantly increased compared to SP, which may improve the quality of spermatozoa in mice by its antioxidant effect, so we hypothesized that Allicin might be one of the active ingredients in GZP for the treatment of asthenozoospermia in mice.

To verify our speculation, we further investigated the mechanism of action of GZP in ameliorating weak spermatogenesis in mice from the perspective of regulating mitochondrial peroxidation and autophagy. The results revealed that GZP significantly scavenged excessive ROS in the testicular tissues of mice with amblyopia, increased mitochondrial membrane potential, inhibited excessive autophagy in mitochondria, and decreased PINK1, Parkin, LC3-I/LC3-II, and Caspase-3 protein expression. Metabolic imbalance, membrane potential alteration, or division abnormality of mitochondria will cause a large release of stimulatory factors (e.g., cytochrome C, ROS, etc.), which will lead to apoptosis. Therefore, the protection of mitochondria plays a crucial role in maintaining the homeostasis of the testicular intracellular environment.

In the present study, the results of mitochondrial structural alterations observed by TEM showed that the mitochondria of testicular tissue cells in mice with weak spermatozoa underwent severe damage and even degradation, indicating that adenine and cyclophosphamide severely damaged the integrity of mitochondria. In the damaged testicular tissue cells, we detected the presence of large amounts of ROS and the occurrence of excessive mitophagy, which may be the underlying cause of the impaired spermatogenesis in testicular tissue. When mice were treated with GZP, ROS were significantly reduced in their testicular tissues, mitophagy was also inhibited, and the repair of damaged mitochondria and abnormal mitophagy of the testis could be clearly seen under TEM. It is concluded that GZP can improve the spermatogenesis of the testis by inhibiting mitophagy in mice testicular tissue cells.

Among the signaling pathways of mitophagy, the most classical one is the PINK1/Parkin pathway, and it has been identified to be used in the detection of autophagosome formation and degradation in mitochondria (26). Under normal physiological conditions, PINK1 is mainly found in the outer membrane of mitochondria, and its content is very low because it is rapidly degraded by protein hydrolases in the outer membrane, but when the mitochondrial membrane potential decreases, protein hydrolases are inhibited, resulting in a large amount of PINK1 accumulating in the damaged mitochondrial outer membrane (27). Parkin is an E3 ubiquitin ligase, which is recruited by PINK1 in the outer membrane and catalyzes the formation and degradation of autophagosomes (28). The ubiquitinated mitochondria are recognized by autophagy-associated protein P62, which promotes the binding of P62 to its cognate proteins on the surface of lysosomal membranes, such as LC3-II, to segregate the defective mitochondria and induce autophagy, thus selectively removing damaged mitochondria and monitoring the quality of the mitochondria, ultimately limiting damage enlargement and inhibiting apoptosis (29). At the same time, autophagy-associated proteins catalyze the transition from cytoplasmic LC3-I to membrane-bound LC3-II, and the LC3-II/LC3-I ratio is often used to reflect the strength of autophagy in cells (30).

Conclusions

In this experiment, we showed that GZP was able to effectively ameliorate asthenozoospermia in mice, and it may inhibit excessive autophagy and protect the integrity of mitochondria by blocking the PINK1/Parkin signaling pathway, and ultimately alleviating the mitochondrial disorders in the testis tissues of mice to inhibit their apoptosis. Our study provides important evidence for the use of *Allium tuberosum Rottler* in the treatment of asthenozoospermia.

Acknowledgments

We would like to thank Dr. Muhammad Shahid Riaz Rajoka for his help in polishing our paper.
Funding: This work was financially supported by National Natural Science Foundation of China (No. 82104398); Administration of Traditional Chinese Medicine 2022 traditional Chinese medicine processing technology inheritance innovation project (No. GZY-KJS-2022-056); and Natural Science Foundation of Chongqing (No.

CSTC2018JCYJ-AX0017).

Footnote

Reporting Checklist: The authors have completed the ARRIVE reporting checklist. Available at https://tau.amegroups.com/article/view/10.21037/tau-24-274/rc

Data Sharing Statement: Available at https://tau.amegroups.com/article/view/10.21037/tau-24-274/dss

Peer Review File: Available at https://tau.amegroups.com/article/view/10.21037/tau-24-274/prf

Conflicts of Interest: All authors have completed the ICMJE uniform disclosure form (available at https://tau.amegroups.com/article/view/10.21037/tau-24-274/coif). The authors have no conflicts of interest to declare.

Ethical Statement: The authors are accountable for all aspects of the work in ensuring that questions related to the accuracy or integrity of any part of the work are appropriately investigated and resolved. Experiments were performed under a project license (No. ZMU21-2306-005) granted by Institutional Animal Ethics Committee of Zunyi Medical University, in compliance with the Laboratory Animal Welfare and Ethics Committee of China.

References

1. Zou C, Xu S, Geng H, et al. Bioinformatics analysis identifies potential hub genes and crucial pathways in the pathogenesis of asthenozoospermia. BMC Med Genomics 2022;15:252.
2. Cavarocchi E, Whitfield M, Saez F, et al. Sperm Ion Transporters and Channels in Human Asthenozoospermia: Genetic Etiology, Lessons from Animal Models, and Clinical Perspectives. Int J Mol Sci 2022;23:3926.
3. Shahrokhi SZ, Salehi P, Alyasin A, et al. Asthenozoospermia: Cellular and molecular contributing factors and treatment strategies. Andrologia 2020;52:e13463.
4. Zhou Y, Yao W, Zhang D, et al. Effectiveness of acupuncture for asthenozoospermia: A protocol for systematic review and meta-analysis. Medicine (Baltimore) 2021;100:e25711.
5. Jin ZR, Fang D, Liu BH, et al. Roles of CatSper channels in the pathogenesis of asthenozoospermia and the therapeutic effects of acupuncture-like treatment on asthenozoospermia. Theranostics 2021;11:2822-44.
6. Zhao Y, Wu J, Li X, et al. Protective effect of Huangqi-Guizhi-Wuwutang against cyclophosphamide-induced spermatogenesis dysfunction in mice by promoting steroid hormone biosynthesis. J Ethnopharmacol 2024;319:117260.
7. Wu X, Chen D, Zhou Y, et al. Efficacy of electroacupuncture for the treatment of asthenozoospermia: A protocol for systematic review and meta-analysis. Medicine (Baltimore) 2021;100:e23350.
8. Yang B, Meng QY, Chen H, et al. Clinical effect of acupuncture combined with traditional Chinese medicine in treatment of oligozoospermia/asthenozoospermia: a meta-analysis. Zhen Ci Yan Jiu 2020;45:243-50.
9. Chen C, Cai J, Ren YH, et al. Antimicrobial activity, chemical composition and mechanism of action of Chinese chive (Allium tuberosum Rottler) extracts. Front Microbiol 2022;13:1028627.
10. Liu N, Hu M, Liang H, et al. Physiological, transcriptomic, and metabolic analyses reveal that mild salinity improves the growth, nutrition, and flavor properties of hydroponic Chinese chive (Allium tuberosum Rottler ex Spr). Front Nutr 2022;9:1000271.
11. Xie B, Wu Q, Wei S, et al. Optimization of Headspace Solid-Phase Micro-Extraction Conditions (HS-SPME) and Identification of Major Volatile Aroma-Active Compounds in Chinese Chive (Allium tuberosum Rottler). Molecules 2022;27:2425.
12. Vringer E, Tait SWG. Mitochondria and cell death-associated inflammation. Cell Death Differ 2023;30:304-12.
13. Nguyen TT, Wei S, Nguyen TH, et al. Mitochondria-associated programmed cell death as a therapeutic target for age-related disease. Exp Mol Med 2023;55:1595-619.
14. Ulloa-Rodríguez P, Figueroa E, Díaz R, et al. Mitochondria in teleost spermatozoa. Mitochondrion 2017;34:49-55.
15. Vertika S, Singh KK, Rajender S. Mitochondria,

spermatogenesis, and male infertility - An update. Mitochondrion 2020;54:26-40.
16. Liu T, Han Y, Zhou T, et al. Mechanisms of ROS-induced mitochondria-dependent apoptosis underlying liquid storage of goat spermatozoa. Aging (Albany NY) 2019;11:7880-98.
17. Piomboni P, Focarelli R, Stendardi A, et al. The role of mitochondria in energy production for human sperm motility. Int J Androl 2012;35:109-24.
18. Li G, Xu Y, Li Y, et al. Qiangjing tablets ameliorate asthenozoospermia via mitochondrial ubiquitination and mitophagy mediated by LKB1/AMPK/ULK1 signaling. Pharm Biol 2023;61:271-80.
19. Voelcker G. Causes and possibilities to circumvent cyclophosphamide toxicity. Anticancer Drugs 2020;31:617-22.
20. Nadeem MS, Kazmi I, Ullah I, et al. Allicin, an Antioxidant and Neuroprotective Agent, Ameliorates Cognitive Impairment. Antioxidants (Basel) 2021;11:87.
21. Shi X, Zhou X, Chu X, et al. Allicin Improves Metabolism in High-Fat Diet-Induced Obese Mice by Modulating the Gut Microbiota. Nutrients 2019;11:2909.
22. Li CL, Liu XH, Qiao Y, et al. Allicin alleviates inflammation of diabetic macroangiopathy via the Nrf2 and NF-kB pathway. Eur J Pharmacol 2020;876:173052.
23. Zhang X, Chen Q. A Twist between ROS and Sperm-Mediated Intergenerational Epigenetic Inheritance. Mol Cell 2020;78:371-3.
24. Barati E, Nikzad H, Karimian M. Oxidative stress and male infertility: current knowledge of pathophysiology and role of antioxidant therapy in disease management. Cell Mol Life Sci 2020;77:93-113.
25. Ribeiro JC, Nogueira-Ferreira R, Amado F, et al. Exploring the Role of Oxidative Stress in Sperm Motility: A Proteomic Network Approach. Antioxid Redox Signal 2022;37:501-20.
26. Tanaka K. The PINK1-Parkin axis: An Overview. Neurosci Res 2020;159:9-15.
27. Gan ZY, Callegari S, Cobbold SA, et al. Activation mechanism of PINK1. Nature 2022;602:328-35.
28. Connelly EM, Frankel KS, Shaw GS. Parkin and mitochondrial signalling. Cell Signal 2023;106:110631.
29. Lu Y, Li Z, Zhang S, et al. Cellular mitophagy: Mechanism, roles in diseases and small molecule pharmacological regulation. Theranostics 2023;13:736-66.
30. Wang S, Long H, Hou L, et al. The mitophagy pathway and its implications in human diseases. Signal Transduct Target Ther 2023;8:304.

Cite this article as: Wu W, Guo X, Li J, Yang M, Xiong Y. Comparison of different processed products of *Allium tuberosum Rottler* for the treatment of mice asthenozoospermia. Transl Androl Urol 2024;13(10):2209-2228. doi: 10.21037/tau-24-274